

Article

# A Tale of Grass and Trees: Characterizing Vegetation Change in Payne's Creek National Park, Belize from 1975 to 2019

Luke Blentlinger \* and Hannah V. Herrero 

Department of Geography, University of Tennessee, 1000 Philip Fulmer Way, Knoxville, TN 37996-0925, USA; hherrero@utk.edu

\* Correspondence: lblentli@vols.utk.edu

Received: 27 May 2020; Accepted: 22 June 2020; Published: 25 June 2020



**Abstract:** The lowland savannas of Belize are important areas to conserve for their biodiversity. This study takes place in Payne's Creek National Park (PCNP) in the southern coastal plain of Belize. PCNP protects diverse terrestrial and coastal ecosystems, unique physical features, and wildlife. A Support Vector Machine (SVM) classification technique was used to classify the heterogeneous landscape of PCNP to characterize woody and non-woody conversion in a time-series of remotely sensed data from 1975, 1993, 2011 and 2019. Results indicate that the SVM classifier performs well in this small savanna landscape (average overall accuracy of 91.9%) with input variables of raw Landsat imagery, the Normalized Difference Vegetation Index (NDVI), elevation, and soil type. Our change trajectory analysis shows that PCNP is a relatively stable landscape, but with certain areas that are prone to multiple conversions in the time-series. Woody vegetation mostly occurs in areas with variable slopes and riparian zones with increased nutrient availability. This study does not show extensive woody conversion in PCNP, contrary to widespread woody encroachment that is occurring in savannas on other continents. These high-performing SVM classification maps and future studies will be an important resource of information on Central American savanna vegetation dynamics for savanna scientists and land managers that use adaptive management for ecosystem preservation.

**Keywords:** remote sensing; neotropical savannas; woody conversion; support vector machine classification; land cover change; protected areas; Payne's Creek National Park

## 1. Introduction

Savannas are mixed woodland–grassland ecosystems with continuous grass cover and variable tree density that can border closed tropical forests. The tropical savanna climate, characterized by its distinct wet and dry seasons, and corresponding ecoregions broadly occupies the space between the equatorial tropical rainforests and subtropical deserts [1,2]. Covering about 20% of the Earth's land surface, savannas account for 30% of terrestrial net primary production [3]. The composition of savanna vegetation is some combination of grassland and sporadic woodland in a patchwork mosaic. The factors that determine boundaries between savanna and forest have generated debate [4]. It has been suggested that the factors that control savanna distribution is variable between continents [3] and that the globally ubiquitous woody encroachment occurring in savannas also varies at continental and regional scales [5]. The determinants of savanna vegetation also vary at regional and local scales [6]. Climate is the primary driver of the distribution of savanna vegetation, especially at continental and regional scales, while topography, soil, fire, and herbivory vary in influence regionally to locally [6].

In some global remote sensing studies, tropical savannas are broadly divided into those that occur in South America, Africa and Australia [3,7,8], possibly because they occupy large areas and are

widely classified as savanna (or associated ecoregions) in publicly available datasets, such as the World Wildlife Fund ecoregions [9]. Global studies provide valuable information on the broad distribution, drivers, and health of savanna vegetation on a continental scale. While vast savannas are widely studied and are included in global studies, smaller pockets of savanna have received less attention. There is a lack of understanding of the fine-scale drivers of the heterogeneous nature of savanna vegetation [10]. Vegetation and soil studies in the expansive Brazilian Cerrado have concluded that fine-scale interactions between vegetation and available water [10], and vegetation and soils [11], are key to understanding neotropical savanna vegetation dynamics. Since knowledge of local dynamics is crucial for understanding the larger savanna landscape, investigating vegetation drivers in smaller pockets of savanna can also contribute to the larger understanding of savannas. Smaller savannas are also key components in the preservation of biodiversity and contributions to the economy via tourism [12]. The exclusion of relatively small savannas from global or continental remote sensing studies can be partly attributed to the use of sensors with large spatial resolutions (e.g., Advanced Very High Resolution Radiometer with 4 km pixel size) that contain much intra-pixel variability. For small study areas that focus on localized savanna vegetation dynamics, finer spatial resolution imagery is necessary to sufficiently characterize the area and the heterogeneous vegetation gradients that are characteristic of savanna landscapes. Even when using imagery from sensors with finer spatial resolution, defining the limits of vegetation in savannas is challenging due to the randomness and spatial heterogeneity of the landscape [13].

Another challenge is that savanna vegetation exists in varying compositions and gradients, and one of the most common ways to assess savanna vegetation with remote sensing is to create discrete land cover classes using an unsupervised or supervised technique [14]. These techniques use a set of variables (inputs) to break each pixel in an image into distinct classes (output). Discrete classifications are simple to understand but prevent variation within classes, which, especially for savannas, can result in an inaccurate representation of the continuous and varied transitions between vegetation. The complicated nature of applying classification techniques to remotely sensed imagery in small savanna landscapes suggests that statistically robust methods should be used. Many common supervised classification techniques, such as Maximum Likelihood, function on the assumption that the statistics for each class are normally distributed and then calculate the probability that a pixel belongs to a specific class [15,16]. Since savanna landscapes often do not fit this definition of normality, such a classification technique is inappropriate. One method to improve supervised classification performance in savanna landscapes is to use non-parametric machine-learning algorithms that do not make assumptions about the distribution of the data, such as Support Vector Machine (SVM) or Random Forest [17,18]. Both SVM and Random Forest have been used to generate high-performing vegetation classifications in some African savanna landscapes [12,19,20].

Savannas in the neotropics cover approximately two million km<sup>2</sup>, or 40% of all land area in the ecozone [21,22]. Of these, the South American savannas (e.g., Brazilian “Cerrado” and nearby Bolivian “Llanos”, Venezuelan-Colombian “Llanos”, etc.) have gained the most attention due to their vastness, high biodiversity and biomass, and global importance in the carbon cycle [21]. While these large savanna expanses are undoubtedly important areas of study, smaller landscapes combined with other information can allow researchers to better understand local drivers of vegetation, such as the influence of topography, soil properties, and disturbances. There are isolated savannas in Central America and the Caribbean that occur above and below 1000 m elevation [23]. While all savannas are in part determined by climatic factors, these savannas are heavily influenced by the underlying physical geography. The upland savannas are characterized by weathered soils, fluvial downcutting and riparian forests, and cooler-weather grasses. The lowland savannas are generally located in flat coastal plains and are created by the interaction between climate, topography, drainage, and soils. Both the upland and lowland savannas are also characterized by disturbance in the form of fire and hurricanes [23]. These large areas, underlain by nutrient-poor soil, have resulted in a general lack of human land use since the times of the Maya.

More recently, some of these savannas have been designated as protected areas for reasons ranging from biodiversity to economics. National parks and other protected areas are ideal for analyzing localized vegetation dynamics for a variety of reasons. Protected areas theoretically act as a static feature in dynamic human-influenced landscapes, and represent a more natural state of being in a given biome [24]. Garbulsky and Paruelo [25] used remote sensing techniques in Argentinian protected areas to derive the “baseline/reference” conditions of various ecosystems as to better assess the impacts of land use and global change. Protected areas act as areas of preservation for biodiversity, and this attracts tourism to boost the economy [12]. In addition, protected areas are often small enough that moderate or fine spatial resolution remotely sensed data is appropriate for an analysis of fine-scale vegetation drivers. Nevertheless, even when coarse imagery is most appropriate, imagery with finer spatial resolution may be able to supplement the analysis. Despite the name, many protected areas are heavily influenced by human involvement or have been in the past. Josefsson et al. [26] used paleoecological and archaeological evidence of long-term human land use in boreal forest protected areas to denounce the notion that purportedly “pristine” forests can be used as ecological references. Hence, protected areas may be an indicator of how local, regional, and global human-environment interactions have affected floral and faunal life in the past and present. This reinforces the need to consider multiple lines of evidence to ascertain the drivers of vegetation change in any landscape [5]. Finally, protected areas are often managed by governments or non-governmental organizations, which means that there are often concerted efforts to maintain and protect the vegetation within a protected area. For example, April Sahara et al. [27] used dendrochronological and remote sensing techniques to characterize woody encroachment over the past 150 years in a pine savanna in Redwood National Park, California. Using their findings, they created models to predict the spatiotemporal characteristics of future woody encroachment in the park [27].

This research was carried out in Payne’s Creek National Park (PCNP) located in the southern coastal plain of Belize. The purpose of this study is to use remotely sensed data to quantify vegetation land cover change from 1975 to 2019, specifically to determine if there has been any woody conversion, as seen in other savanna landscapes globally. This study addresses the following questions: (1) Can a SVM accurately classify the complex savanna landscape of PCNP over time? (2) What is the overall pattern of woody and non-woody conversion in PCNP from 1975 to 2019 using the SVM classifications? (3) What are the fine-scale variables linked to vegetation distribution in PCNP?

## 2. Materials and Methods

### 2.1. Study Area

Payne’s Creek National Park (PCNP) in the Toledo District of southern Belize covers approximately 152 km<sup>2</sup> of low elevation land that borders the Caribbean Sea (Figure 1). The park is located at approximately 16.3° N 88.6° W in Belize’s southern coastal plain. Belize has a subtropical to tropical climate with mean monthly minimum/maximum temperatures from 16/28 °C in winter to 24/33 °C in summer [28]. The Köppen climate classification of most of Belize, including PCNP, is “tropical monsoon” [29], which is characterized by a distinct wet and dry season. The majority of rainfall falls from June to November in Belize [29]. For this study, the dry season is considered as January–May and the wet season is June–December. The dry season average precipitation in PCNP is approximately 498 mm and 2208 mm in the wet season. The minimum/maximum precipitation in PCNP in the dry season was 269 mm/790 mm (1987/1990) and 1647 mm/2903 mm (2004/1979) in the wet season [30–32]. Mean annual rainfall ranges from 1524 mm in the north and 4064 mm in the south. This variability occurs due to orographic lifting over steep slopes and the seasonal migration of the Inter-Tropical Convergence Zone [29]. Belize contains upland savannas known as the Mountain Pine Ridge and lowland savannas of the northern and southern coastal plains. This study focuses on Belize’s lowland savannas.

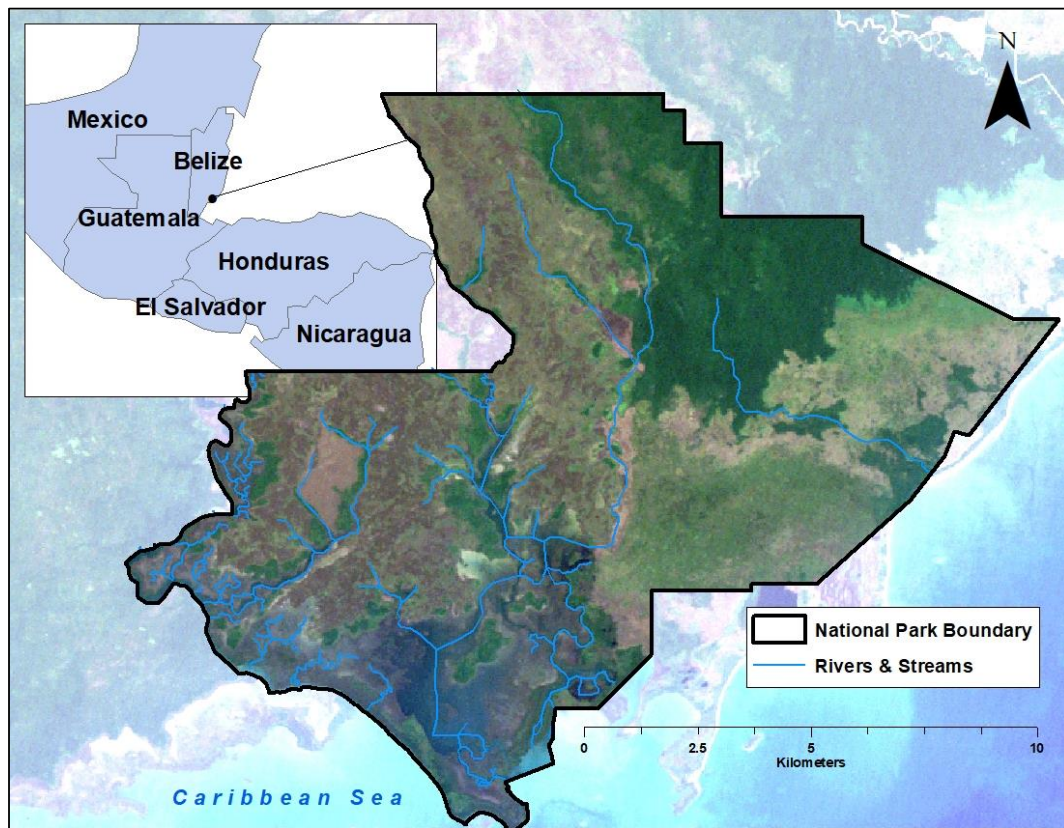


**Figure 1.** Map of Payne's Creek National Park (PCNP), showing nearby countries in Central America. Image of PCNP is a true color composite from Landsat 5 TM taken in March 2011. Shapefile of Central America from Natural Earth. Shapefile of Belize and its rivers from Biodiversity and Environmental Resource Data System of Belize. Shapefile of Payne's Creek National Park from Protected Planet.

The lowland savannas of Belize are located between dense broadleaf rainforests inland and mangrove swamps seaward in the relatively flat, poorly drained coastal plain [33]. Vegetation in these savannas are a mosaic of grassland and pine or oak trees, and pockets of broadleaf forest [23,28,34]. Both upland and lowland savannas are in areas with weathered, acidic and nutrient-poor soils, but the upland savannas are well-drained while those in the lowlands frequently experience flooding and drying with the wet and dry seasons, respectively [35]. The lowland area is underlain by the Yucatan limestone platform, which was shallow sea during the Pliocene (2–13 Myr BP). Subsurface clay sits atop the limestone platform, resulting in widespread poor drainage in the lowlands. Sands and gravels from the nearby Maya Mountains eroded and accumulated on the clay and formed the current lowland coastal plain [35]. Savannas in the low-lying area usually occur on nutrient-poor soils underlain by the sands and gravels [28]. Undulations in the lowland topography result in improved drainage and the dominance of woody vegetation, such as pine and oak. Dense broadleaf forests occur along rivers in the area due to increased nutrients in alluvial deposits originating in the Maya Mountains [28]. At an even finer scale, disturbance feedbacks in the form of fire and hurricanes control the boundaries between grasses and trees. This is partly because the dominant pine species, *Pinus caribaea*, most readily regenerates on sunlit mineral soils. These soils become available after fire from the removal of grass cover and organic matter, or because old trees are killed and stand density is reduced [36]. Similarly, strong winds from hurricanes can reduce stand density and allow sunlight to penetrate to the surface [36]. The Toledo Institute for Development and Environment (TIDE) manages PCNP and uses fire management practices in the fire-adapted tropical pine savanna and grassland ecosystems. While the pine savanna is fire adapted, too many fires would eventually lead to a grassland without pine by scorching saplings attempting to regenerate. Too few fires results in a thick herbaceous layer

and succession towards broadleaf forest. One result of less pine is habitat loss for the endangered yellow-headed parrot, *Amazona oratrix*, which uses pine trees to nest [37]. Since the pine savanna and yellow-headed parrot are both endangered and reliant on fire, TIDE places a high priority on fire management in PCNP.

According to the ecosystem classifications created by other researchers [33,38], PCNP contains open savanna, dense tree savanna, forest inclusion (within open savanna), forest, mangrove and littoral swamp, and wetland. Open savanna is dominated by grasses and sedges with semi-open to very open areas of pine, oak, palmetto and craboo. Dense tree savanna is the transitional area from forest or forest inclusion to open savanna. Elevation broadly distributes the wetland in the lowest lying areas and forest in the higher elevations (<35 m), with savanna in between. The mangrove and littoral swamps are on the coast and also extend inland, beyond the mouth of Payne’s Creek and other streams.

### 2.2. Climate Data

Climate data was used to avoid anomalies and assess the viability of carrying out dry-season vegetation classification and change trajectory analysis in the months from which the imagery was collected. We used two sources of historical climate data to encompass the entire time period. The Climate Hazards Group InfraRed Precipitation with Station Data (CHIRPS) from the University of California Santa Barbara is a quasi-global rainfall dataset that spans 50° S–50° N across all longitudes. CHIRPS uses 0.05° resolution satellite imagery and in-situ station data to produce a gridded, monthly dataset the spans from 1981 to near-present [32]. Since the remote sensing analysis contains the earliest usable Landsat imagery of PCNP from 1975, the CHIRPS data does not encompass the earliest part of the study period. WorldClim is another gridded dataset for historical climate data. Specifically, the CRU-TS 4.03 [31] downscaled with WorldClim 2.1 [30] is a monthly climate dataset for global land areas at approximately 21 km spatial resolution. Since this dataset provides climate data that extends back to 1960, it was used to extend our climate data back to 1970. Even though the CHIRPS and WorldClim data are at different spatial resolutions, both were used to assess the climate in PCNP. Based on the 49 years of combined CHIRPS and WorldClim precipitation data, the dry season (January–May) average precipitation in PCNP is approximately 498 mm and 2208 mm in the wet season [30–32]. Figure 2, which shows the yearly cumulative precipitation Z-scores for the CHIRPS and WorldClim data from 1970 to 2018, was used to assess which years were drier or wetter than average precipitation in PCNP to ensure that anomalous years of imagery were not chosen for analysis.

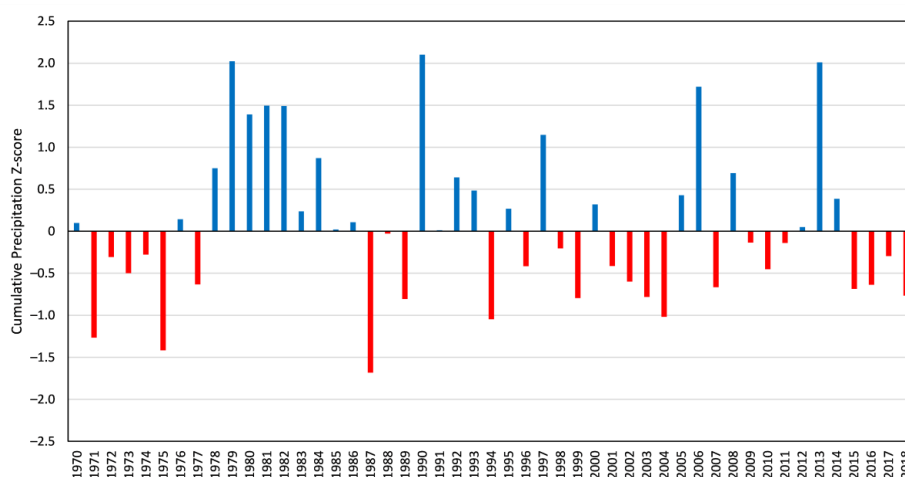


**Figure 2.** Total annual rainfall Z-scores for PCNP from 1981 to 2019. Rainfall data from WorldClim and CHIRPS.

### 2.3. Data and Image Analysis

#### 2.3.1. Remotely Sensed Data

This study used remotely sensed Landsat Multispectral Scanner (MSS), Thematic Mapper (TM), and Operational Land Imager/Thermal Infrared Sensor (OLI/TIRS) imagery to create land cover classification and change trajectories and carry out Normalized Difference Vegetation Index (NDVI) analysis on freely available imagery from four years in the dry season: 1975, 1993, 2011 and 2019. Landsat imagery was chosen for this analysis for its relatively fine spatial resolution and its long-term database of publicly available satellite imagery. All Landsat imagery was obtained from the United States Geological Survey Earth Explorer and came atmospherically and geometrically corrected [39]. The images from March 1975 and March 2011 are completely cloud-free, while those from March 1993 and January 2019 have some clouds and cloud shadows, which were masked out. The MSS data (bands 1–4), obtained by Landsat-2 in 1975 at 80 m spatial resolution, were resampled to 30 m pixel size to align with the resolution of the TM (bands 1–7) and OLI/TIRS (bands 1–8, 10, 11) imagery from Landsats 4, 5 and 8 (1993, 2011 and 2019). All raw image bands (except OLI band 9) were subset to a shapefile of PCNP obtained from Protected Planet and were used in the classification analysis. Additionally, the three other layers outlined in Section 2.3.2 below were created or obtained to be used as variables in the SVM classification.

#### 2.3.2. Other Data: Normalized Difference Vegetation Index (NDVI), Digital Elevation Model (DEM), and Soil Type

NDVI is a commonly used vegetation index that has a variety of applications, but its inherent use is to quantify and discriminate vegetation characteristics [40]. The calculation for NDVI is:

$$NDVI = \frac{NIR - Red}{NIR + Red}$$

where *NIR* is near infrared reflectance and *Red* is red reflectance in the electromagnetic spectrum. NDVI is an indicator of vegetation productivity and degradation [40,41]. Using band math tools in the Environment for Visualizing Images (ENVI) 5.5 software, four NDVI maps, one for each image in the time series, was created from the *NIR* and red bands to be used as an input variable (Figure 3).

As was previously stated, edaphic factors are key to understanding the distribution of woody and non-woody vegetation in the lowland savannas of Belize. Nutrient-poor soils in the Belize lowlands stem from inundations in the wet season due to poor drainage from subsurface clay and intense desiccation in the dry season [35]. Higher elevations and variable slopes can result in locally improved drainage and the opportunity for soil development and woody vegetation establishment. To encompass the importance of topography in the classification, a 30 m digital elevation model (DEM) from the USGS Shuttle Radar Topography Mission (SRTM) was included (Figure 3). The DEM was acquired from the USGS Earth Explorer website and the study area was subset in ArcMap 10.7.1 using the PCNP shapefile.

While the subsurface clay in PCNP affects vegetation through seasonal inundations, the soil types that overlay the clay also affect vegetation distribution. Alluvial deposits along rivers and streams, for example, are nutrient rich and promote woody growth compared to the Maya Mountain outwash that underly the grasslands [28]. To incorporate the importance of soil type in the classification, a Belize soils map created by the Selva Maya consortium (Figure 3) was included as a variable [42].

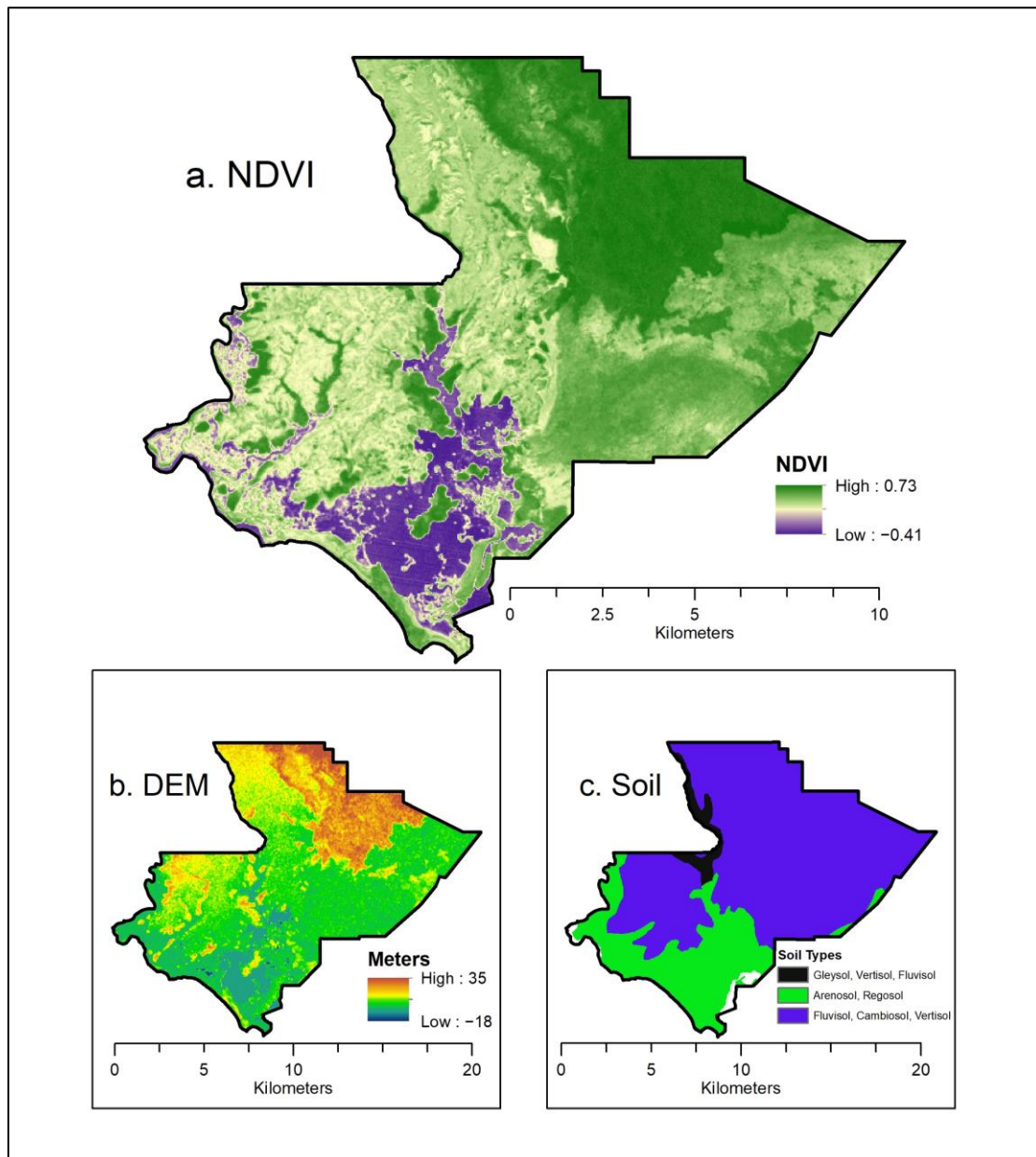


**Figure 3.** Maps of data used as variables in the Support Vector Machine (SVM) classification: (a) Normalized Difference Vegetation Index (NDVI) map of Landsat-5 Thematic Mapper (TM) image from March 2011; (b) Shuttle Radar Topography Mission (SRTM) Digital Elevation Model (DEM) showing elevation in meters of PCNP, from United States Geological Survey (USGS) Earth Explorer; (c) soil type map showing areas in PCNP with differing major soil types, from Selva Maya consortium.

#### 2.4. Land Cover Classification and Change

##### 2.4.1. Land Cover Classes

Other research carried out in Belize, including the southern coastal plain, identify the dominant land covers of PCNP as open savanna, dense tree savanna, forest and wetland [28,33]. The open savanna classification is characterized by the domination of grasses and sedges with scattered trees and shrubs. Similarly, the species composition of the dense tree savanna is essentially the same as the open savanna, but with semi-closed oak and pine canopies. The forest land cover includes lowland broad-leaved wet forests, lowland broad-leaved moist scrub forests, and mangrove and littoral forests.

Wetland land cover in PCNP are comprised of tall herb lowland swamp and *Eleocharis* marshes [33,34]. The focus of this study, however, is to characterize conversion to and from woody and non-woody vegetation over time, so the land cover classes used in this classification are more general: forest, grass, wetland, and water.

#### 2.4.2. Training Data

Since fieldwork was not undertaken, all training and testing data in this study were collected via easily accessible high-resolution satellite imagery. Using the “Generate Random Points” tool in ArcMap, random points were generated throughout the PCNP shapefile. Using imagery from Google Earth and the ArcGIS satellite basemap, the random points were identified as belonging to one of the four training sample categories: forest, grass, wetland, or water. The 2017 update of the Belize Ecosystems map from Meerman and Sabido [38] and the Savanna Ecosystems Map of Belize from Bridgewater et al. [33] were used to aid in the spectral differentiation of classes. Additional classes for clouds and cloud shadows were used in the images from 1993 and 2011. A total of 198 points comprised the training dataset, with 133 of those being for the four land cover classes and 65 for clouds and shadows. Approximately 80% of the samples were used to train the classifier and 20% were saved for accuracy assessment [12]. The training and testing data were randomly split by the “Subset Features” tool in ArcMap.

#### 2.4.3. Support Vector Machine Classification

A radial basis function kernel SVM was chosen for these classification maps due to the capability of the classifier to distinguish non-linear boundaries between classes, especially when training data sample size is low. The SVM classifier is a supervised classification technique that uses statistical learning to discriminate classes by maximizing the separation between discrete classes based on training data. The optimal separating hyperplane refers to this boundary, which maximizes class separation and minimizes misclassification [43,44].

The SVM classification was carried out in ENVI 5.5 using a radial basis function (RBF) kernel. The four classifications were carried out on dry season images using Landsat-2 MSS bands 1–4 for March 1975, Landsat-4 TM bands 1–7 for March 1993, Landsat-5 TM band 1–7 for March 2011, and Landsat-8 OLI/TIRS bands 1–8, 10 and 11 for January 2019 imagery. All four classifications also included the derived NDVI using the NIR and Red bands, the SRTM DEM, and the Belize Soils Map. The raw Landsat bands, NDVI, DEM and Belize Soils Map were all subset to the PCNP shapefile in ArcMap and stacked together as a multi-band file in ENVI. Accuracy assessments were performed in ENVI for all four classification maps using ground truth regions of interest.

#### 2.4.4. Change Detection

The first step for detecting conversions to and from woody and non-woody vegetation was to simplify the land cover classes. Using the “Reclassify” tool in ArcMap 10.7.1, the forest class pixels were reclassified as “Woody” while grass, wetland, and water were reclassified as “Non-Woody.” The cloud and cloud shadow pixels were reclassified to no data. After all maps were reclassified, we used the ArcMap “Raster Calculator” to create change trajectories. A change trajectory was created for all four dates to characterize overall woody and non-woody conversions in the time-series. Three additional change trajectories were created to show woody and non-woody conversion between 1975 and 1993, 1993 and 2011, and 2011 and 2019.

### 3. Results

#### 3.1. Land Cover Classification and Change Trajectories

##### 3.1.1. Classification Maps

The first output from the SVM classification is a land cover classification map for each of the four dates (Figure 4). These maps show where forest, grass, water, and wetland classes are located in PCNP. The 1993 and 2011 maps also contain cloud and cloud shadow classes. Figure 4 shows that, in all four maps, the four land cover classes are generally grouped together, but with transitional areas between them. Higher elevations and improved drainage promote closed forest in the northeast; seasonal inundations and nutrient-poor soils promote grasses and interspersed trees in the central and western low-lying areas; waterlogged soils promote wetlands in the east that border the grass, closed forest, and Atlantic Ocean to the south; water accumulates and discharges into the Caribbean Sea in the southwest and southeast. The most notable transitions are the more gradual transitions between grass and wetland, forest and wetland, and the quicker transition between grass and forest.

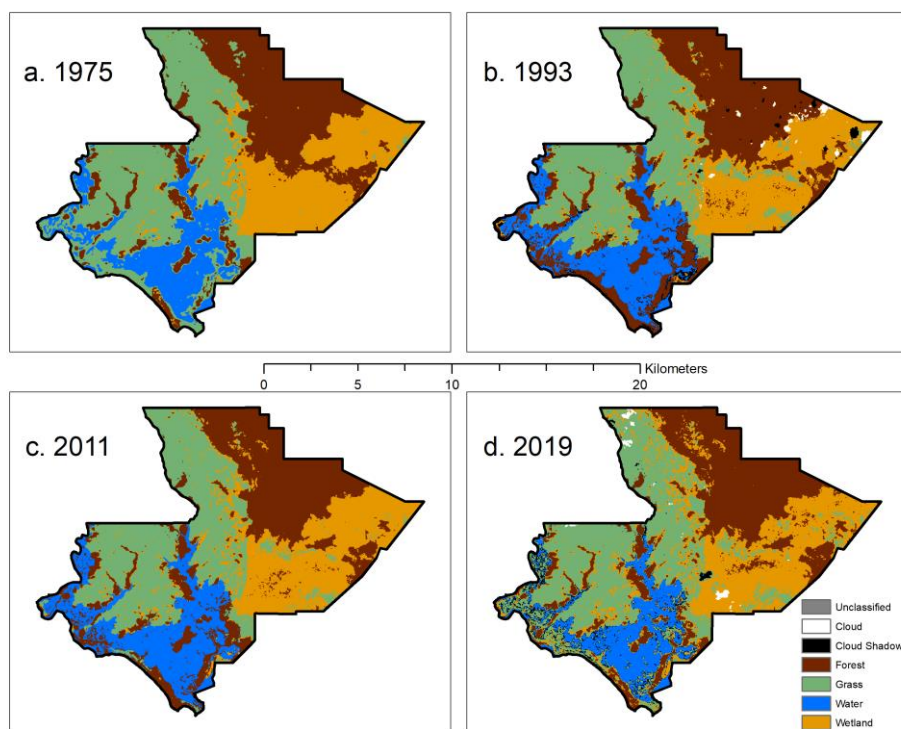


**Figure 4.** Support Vector Machine classification results based on Landsat imagery and other data for: (a) 1975; (b) 1993; (c) 2011; (d) 2019.

The error matrices (Table 1) show where misclassification occurred in the four images. Table 1 also shows class error commission and omission percentages, and overall accuracy and kappa coefficients. The overall accuracy for the 1975, 1993, 2011 and 2019 classifications are 88.5%, 96.9%, 96.2% and 86.1%, respectively, and the kappa statistics are 0.8402, 0.9612, 0.9474 and 0.8289. While the classifications perform well overall, some confusion, especially in the grass and wetland classes, can be noted visually. The transitional areas between grass and wetland are most well defined in the 1975 land cover classification, with each subsequent map having less definition between classes. Another issue for the SVM classifier was differentiating between spectrally similar water and cloud shadow, especially in the 2019 land cover classification; nevertheless, grouping classes together through reclassification results in new classification maps where these issues are less pronounced.

**Table 1.** Error matrices for Support Vector Machine classification results based on Landsat imagery and other data for 1975, 1993, 2011 and 2019. The 1975 and 2011 images were completely cloud-free.

Error Matrix	Forest	Grass	Water	Wetland	Cloud	Cloud Shadow	Total	Class Error Commission %	Class Error Omission %
<b>1975</b>									
Unclassified	0	0	0	0	n/a	n/a	0		
Forest	6	0	0	0	n/a	n/a	6	0.0	0.0
Grass	0	7	2	0	n/a	n/a	9	22.2	12.5
Water	0	0	2	0	n/a	n/a	2	0.0	50.0
Wetland	0	1	0	8	n/a	n/a	9	11.1	0.0
Total	6	8	4	8	n/a	n/a	26		
<b>1993</b>									
Unclassified	0	0	0	0	0	0	0		
Forest	6	0	1	0	0	0	7	14.3	0.0
Grass	0	8	0	0	0	0	8	0.0	0.0
Water	0	0	3	0	0	0	3	0.0	25.0
Wetland	0	0	0	8	0	0	8	0.0	0.0
Cloud	0	0	0	0	3	0	3	0.0	0.0
Cloud Shadow	0	0	0	0	0	3	3	0.0	0.0
Total	6	8	4	8	3	3	32		
<b>2011</b>									
Unclassified	0	0	0	0	n/a	n/a	0		
Forest	6	0	1	0	n/a	n/a	7	14.3	0.0
Grass	0	8	0	0	n/a	n/a	8	0.0	0.0
Water	0	0	3	0	n/a	n/a	3	0.0	25.0
Wetland	0	0	0	8	n/a	n/a	8	0.0	0.0
Total	6	8	4	8	n/a	n/a	26		
<b>2019</b>									
Unclassified	0	0	0	0	0	0	0		
Forest	6	0	0	0	0	0	6	0.0	0.0
Grass	0	7	2	0	0	0	9	22.2	12.5
Water	0	0	2	0	0	0	2	0.0	50.0
Wetland	0	1	0	8	2	0	11	27.3	0.0
Cloud	0	0	0	0	4	0	4	0.0	33.3
Cloud Shadow	0	0	0	0	0	4	4	0.0	0.0
Total	6	8	4	8	6	4	36		
1975 Kappa Coefficient: 0.8402 Overall Accuracy: 88.5%; 1993 Kappa Coefficient: 0.9612 Overall Accuracy: 96.9%;									
2011 Kappa Coefficient: 0.9474 Overall Accuracy: 96.2%; 2019 Kappa Coefficient: 0.8289 Overall Accuracy: 86.1%									

### 3.1.2. Change Trajectories

Figure 5 shows the four SVM classification maps after being reclassified. There is an average of 176,765 reclassified pixels in the four maps with approximately 70% being non-woody and 30% woody. The number of pixels in the four classifications are not equal because of the presence of cloud and cloud shadow pixels in the 1993 and 2011 imagery, which were reclassified as no data. Figure 6 shows the overall change trajectory using all SVM classifications in the time-series. Visually, most pixels did not undergo change, as the WWWW (brown) and NNNN (blue) trajectories represent pixels that, throughout the time-series, remain woody or non-woody, respectively. Table 2 shows that 86.7% of pixels did not undergo conversion throughout the entire time-series, while all other pixels underwent conversion at least once. Of the 13.3% that underwent conversion, 66.3% ended the time-series as non-woody and 33.7% as woody. There are some visually discernible spatial patterns to the conversions that occurred in the overall change trajectory, indicating that some portions of PCNP may be more susceptible to land cover change. Figure 6 shows that changes occurred along the coast in the south and southwest. Conversions also appear to be more frequent on the fringes of the pockets of forest that surround fluvial systems. Substantial change also occurred in the eastern PCNP wetland and within the northern eastern closed forest. It appears that little widespread change occurred in the grasslands, but with pronounced conversions occurring in transition zones between woody and non-woody vegetation.

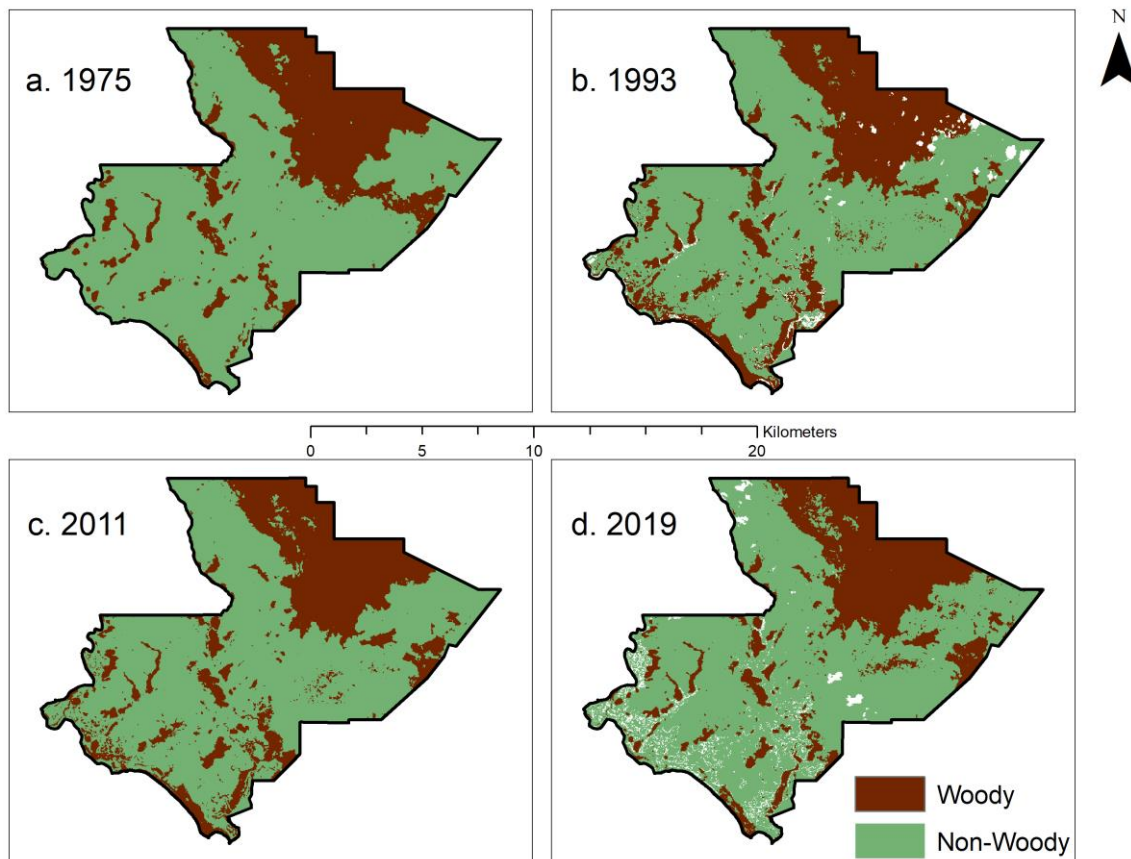


**Figure 5.** Maps showing the SVM land cover classification after reclassifying pixels as “Woody” or “Non-Woody”: (a) 1975; (b) 1993; (c) 2011; (d) 2019. White pixels represent cloud and cloud shadow, which were reclassified as no data.

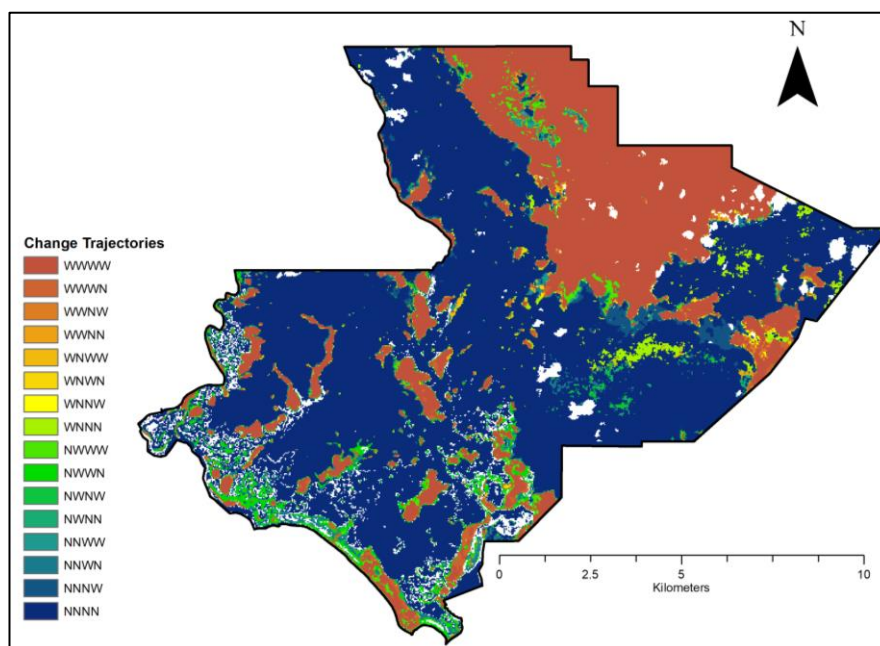


**Figure 6.** Overall change trajectory map using all four (1975, 1993, 2011, 2019) land cover classifications. Woody is “W” and non-woody is “N.” White pixels represent no data.

**Table 2.** SVM classifier change trajectory pixel counts and percent change with explanation of each change trajectory. Woody is “W” and non-woody is “N”.

Trajectory	1975	1993	2011	2019	Pixel Count	% Change
WWWW	W	W	W	W	41296	24.4
WWWN	N	W	W	W	3546	2.1
WWNW	W	N	W	W	398	0.2
WWNN	N	N	W	W	423	0.2
WNWW	W	W	N	W	398	0.2
WNWN	N	W	N	W	418	0.2
WNNW	W	N	N	W	258	0.2
WNNN	N	N	N	W	2134	1.3
NWWW	W	W	W	N	2060	1.2
NWWN	N	W	W	N	4231	2.5
NWNW	W	N	W	N	181	0.1
NWNN	N	N	W	N	1181	0.7
NNWW	W	W	N	N	1172	0.7
NNWN	N	W	N	N	3091	1.8
NNNW	W	N	N	N	2988	1.8
NNNN	N	N	N	N	105445	62.3
<b>Total</b>					169220	100.0

While the overall change trajectory map shows a more holistic view of change in the time-series, showing only the conversions between successive imagery dates allows for highlighting the timing of certain changes. Figure 7 shows three change trajectories which highlight woody and non-woody conversions between adjacent imagery dates. These maps make the timing of certain conversions much clearer. The conversions between 1975 and 1993 are perhaps the most distinct, with the south and southwest portions of PCNP undergoing widespread woody conversion (colored in yellow) along the coast. Non-woody conversion (green) occurred in the east in the transition from forest to wetland, indicating that these pixels may have converted from forest to wetland. Table 3 shows that 6.6% of all pixels converted to woody vegetation between 1975 and 1993, which is the highest rate of woody conversion between all four imagery dates. The 2.2% conversion to non-woody land cover between 1975 and 1993 is the lowest of the three change trajectories. Between 1993 and 2011, more than 95% of all pixels underwent no change and 3% converted to non-woody. Spatially, most of this change occurred along the coast, but there are also non-woody conversions within the grassland, wetland, and closed forest, especially in transitional areas. The conversions that occurred between 2011 and 2019 were mostly non-woody and appear to be in areas that had already undergone conversion at other points in the time-series.

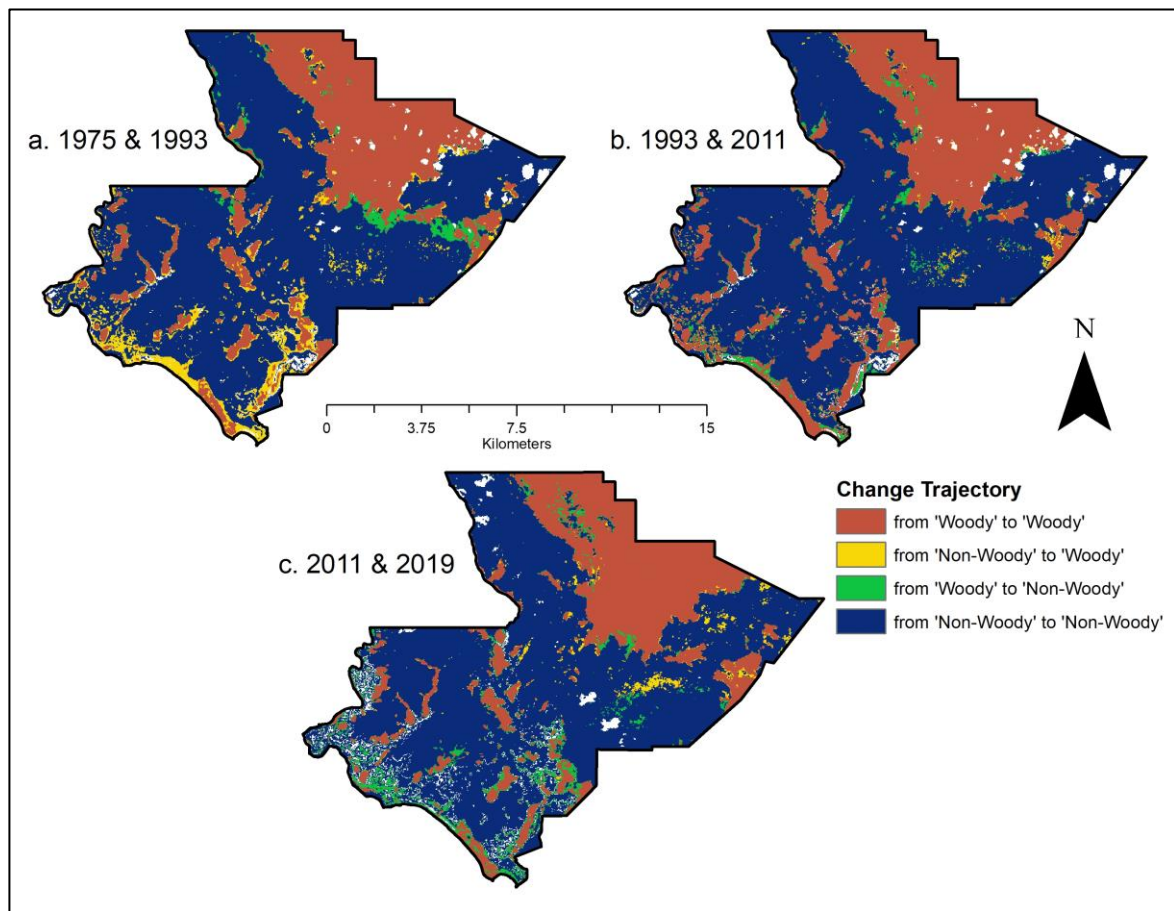


**Figure 7.** Change trajectory maps for successive imagery dates: (a) 1975 and 1993; (b) 1993 and 2011; (c) 2011 and 2019. White pixels represent no data.

**Table 3.** Change trajectory percent changes between successive imagery dates.

Trajectory	SVM Classifier % Change		
	1975–1993	1993–2011	2011–2019
Non-Woody to Woody	6.6	1.3	1.9
No Change	91.2	95.7	93.3
Woody to Non-Woody	2.2	3.0	4.8
<b>Total</b>	<b>100.0</b>	<b>100.0</b>	<b>100.0</b>

#### 4. Discussion

This study demonstrates a novel application of a non-parametric supervised classification technique in a heterogeneous neotropical savanna landscape. SVM classifiers are especially useful when training data is limited and boundaries between classes are not abrupt, which are both true for this study. The SVM classification of the heterogeneous landscape in PCNP is high-performing and performs similarly to other studies that use SVM to classify savanna vegetation [19,45,46]. This research adds to the growing recognition of the robustness of SVM classifiers in savannas and other heterogeneous landscapes. The use of SVM needs to be explored further in savanna landscapes, especially in other small Central American savannas that are underrepresented in regional and global studies. Understanding conversions to and from woody and non-woody vegetation is a simple, but important way for researchers and land managers to compartmentalize and interpret change occurring on a landscape. This streamlined view of vegetation change is especially useful in savanna landscapes, which contain grass and trees in alternative stable states that are constantly experiencing change driven

by disturbances and feedbacks [6]. Understanding where land conversions are occurring in savanna and adjacent landscapes is crucial so that managers can investigate the source of change and determine if planning and intervention is needed or if the change is part of the overall function of the ecosystem.

Our analysis reveals a relatively stable landscape in PCNP, but with spatially concentrated areas that are prone to vegetation conversion. The overall change trajectory (Figure 6, Table 2) does not reveal evidence of widespread woody or non-woody conversion in PCNP from 1975 to 2019. This finding is notable because it differs from studies of savanna vegetation dynamics on other continents. In sub-Saharan Africa, remote sensing studies have found evidence of woody encroachment in savannas [12,20]. The authors of [47] reviewed 16 studies that present evidence of woody encroachment and supplement those findings with continental-scale remote sensing analysis. Moreover, at a continental scale, a connection between mean annual precipitation and woody encroachment was discovered by the authors of [48], who also suggested that future increases of water availability in African Savannas could lead to enhanced woody conversion. In a protected area in northern Australia, researchers found forest expansion and grassland contraction in a lowland Eucalyptus savanna [49]. Further evidence of tropical rain forest expansion into savanna was found across multiple sites in northeast Australia, most likely attributed to increased atmospheric CO<sub>2</sub> [50]. In South America, it has been suggested that the expansion of riparian forests within the Brazilian Cerrado savannas has been occurring for thousands of years and will continue to do so with modern climate change [51]. Based on an extensive review covering 112 savanna sites, the authors of [5] conclude that widespread woody encroachment is occurring in savannas across Africa, Australia, and South America; however, regionally specific characteristics of plant biology, land use, disturbance, moisture availability, soil nutrients, etc. determine encroachment susceptibility for the landscape.

Figure 7 shows where conversions occurred between imagery dates and reveals that certain areas in PCNP are especially sensitive to change and have changed multiple times. These sensitive areas are along the coast and the transition zones between forest, grassland, and wetland. We hypothesize that some of these areas are especially susceptible to conversion due to disturbance and the inherent sensitivity and heterogeneity of vegetation transition zones in savannas. Clusters of conversion to non-woody vegetation (colored in green) between 1975 and 1993 may be a result of selective logging of broadleaf and pine trees, which occurred until becoming a protected area in 1994 [52]. Later in the time-series, non-woody conversions surrounding pockets of forest could be a result of fire management practices. TIDE uses prescribed fires in PCNP to maintain the pine savanna and promote post-fire pine regeneration. If the fire management efforts were not effective, it is likely that the 1993–2011 and 2011–2019 change trajectories would show an expansion of non-woody vegetation or woody encroachment in the grassland [52].

Between 1975 and 1993, there is also an area of concentrated woody conversion (colored in yellow) that occurs along the PCNP coastline. Meerman and Sabido [2001] indicate that this coastal area contains mangrove and littoral forest. Mangrove and littoral forest are dynamic environments that occupy the space between marine and terrestrial ecosystems, so it is not surprising that the PCNP coastline has experienced change in the time-series. Nevertheless, the spatially concentrated woody conversion along the coast suggests that a disturbance event, such as a hurricane or wildfire, or its aftermath could be the source of change. Since this is a forest in the littoral zone, pre-1975 hurricane activity is more likely to have damaged the mangroves or reduced stand density. There were multiple tropical cyclone events that affected Belize before 1975: Hurricane Hattie (1961), Hurricane Francelia (1969), Hurricane Edith (1971), Tropical Storm Laura (1971), and Hurricane Fifi (1974) [53]. Stoddart [54] observed mangrove defoliation and widespread destruction of coconut palms in areas affected by Hurricane Hattie [54]. These pre-1975 events may have reduced littoral forest density and induced regrowth. The fact that there are also groups of pixels along the coast that went from woody to woody between 1975 and 1993 suggests that woody conversion was already happening before 1975 and continued through 1993. Even though mangrove forests are not typically associated with savanna

landscapes, the importance of the mangroves to the pine savanna manifests through the interception of energy from hurricanes and other storms [55].

One of the contributions of this study to savanna science is the importance of ascertaining and including fine-scale driving factors, such as topography and soil type, into remote sensing analyses. Each savanna landscape is unique and contains varying drivers and disturbances that determine vegetation distribution, with common drivers often being plant available moisture and nutrients [56]. In the lowland savannas of Belize, edaphic and topographic factors play key roles in vegetation distribution [23]. These factors vary on multiple scales in Belize, and the fine-scale variations within these are important vegetation drivers in PCNP. Elevation ranges from 35 m to sea level and broadly distributes vegetation in PCNP; nevertheless, it appears that the fine-scale consequences of elevation, such as locally improved drainage, determine where woody vegetation can survive. Since there are widespread nutrient-poor soils in the coastal plain, pockets of nutrient rich, alluvial soils along fluvial systems also determine the extent to which woody vegetation can establish. As is seen in the SVM classification maps, pixels at higher elevations and around fluvial systems were classified as woody vegetation, which agrees with other studies [28,33,38]. These results parallel the findings of a study in Kenya by Coughenour and Ellis [57]. They determined that water availability and physical landscape pattern control the distribution of grass and trees, as woody vegetation almost only occurred in riparian zones. It was concluded that there is a hierarchy of physical factors that determine where woody vegetation can develop on this landscape at multiple scales: climate at regional and continental, topographic influence on water redistribution and the geomorphic effect on soil moisture regionally, and water redistribution and disturbance at the local scale [57]. Similarly, the interaction between rainfall and topography distribute vegetation in the Serengeti-Maasai Mara savanna ecosystem [58]. Including the SRTM DEM and the soils map as variables in the SVM classifications were paramount in encompassing “bottom-up” drivers of woody and non-woody vegetation distribution that remotely sensed imagery alone cannot include. Future vegetation studies in PCNP should quantitatively describe the influence of riparian zones and alluvium on woody vegetation distribution.

## 5. Conclusions

The research presented here demonstrates that a non-parametric supervised land cover classification technique performs well in this heterogenous savanna landscape. Using a SVM classification and time-series change trajectories, we characterized woody and non-woody conversion in PCNP from 1975 to 2019 and found a relatively stable landscape. Our land cover classification revealed that some portions of PCNP that are susceptible to change tend to be in areas where the dominant vegetation cover is transitioning. These areas overlap with changes in elevation and/or riparian zones, indicating the importance of slight variations in drainage and nutrient availability. Consequently, our analysis suggests that topo-edaphic factors play a key role in controlling woody biomass in PCNP, and future studies should explore this further. We attribute the other areas with similarly grouped conversions to be disturbance or human induced, such as fire, hurricane-induced vegetation damage, or logging. Unlike many other savanna landscapes, woody encroachment is not widespread in PCNP.

The findings from this study have important implications for savanna scientists and land managers in Belize, such as a better understanding of fine-scale savanna vegetation drivers and areas susceptible to vegetation conversion. Adding to the knowledge of how this landscape functions will allow land managers to improve their efforts of protecting the pine savanna and its associated wildlife. Future work should improve the vegetation classification with field validation, quantitatively relate topo-edaphic factors to vegetation conversion, and compare these findings to other Central American savannas.

**Author Contributions:** Conceptualization, L.B. and H.V.H; methodology, L.B. and H.V.H; software, L.B.; formal analysis, L.B.; investigation, L.B.; resources, L.B.; data curation, L.B. and H.V.H; writing—original draft preparation, L.B.; writing—review and editing, L.B. and H.V.H; visualization, L.B.; supervision, H.V.H.; project administration, H.V.H. All authors have read and agreed to the published version of the manuscript.

**Funding:** This research received no external funding.

**Acknowledgments:** We would like to thank Cathy Smith for introducing us to this landscape and Michael Dobbins for providing insight about the study area.

**Conflicts of Interest:** The authors declare no conflict of interest.

## References

1. Kottek, M.; Grieser, J.; Beck, C.; Rudolf, B.; Rubel, F. World Map of the Köppen-Geiger climate classification updated. *METZ* **2006**, *15*, 259–263. [CrossRef]
2. Chapin, F.S.; Matson, P.A.; Vitousek, P. *Principles of Terrestrial Ecosystem Ecology*; Springer Science & Business Media: Berlin/Heidelberg, Germany, 2011; ISBN 978-1-4419-9504-9.
3. Lehmann, C.E.R.; Anderson, T.M.; Sankaran, M.; Higgins, S.I.; Archibald, S.; Hoffmann, W.A.; Hanan, N.P.; Williams, R.J.; Fensham, R.J.; Felfili, J.; et al. Savanna Vegetation-Fire-Climate Relationships Differ Among Continents. *Science* **2014**, *343*, 548–552. [CrossRef]
4. Cole, M.M. The savannas. *Prog. Phys. Geogr. Earth Environ.* **1987**, *11*, 334–355. [CrossRef]
5. Stevens, N.; Lehmann, C.E.R.; Murphy, B.P.; Durigan, G. Savanna woody encroachment is widespread across three continents. *Glob. Chang. Biol.* **2017**, *23*, 235–244. [CrossRef]
6. Murphy, B.P.; Bowman, D.M.J.S. What controls the distribution of tropical forest and savanna? *Ecol. Lett.* **2012**, *15*, 748–758. [CrossRef] [PubMed]
7. Staver, A.C.; Archibald, S.; Levin, S.A. The Global Extent and Determinants of Savanna and Forest as Alternative Biome States. *Science* **2011**, *334*, 230–232. [CrossRef] [PubMed]
8. Southworth, J.; Zhu, L.; Bunting, E.; Ryan, S.J.; Herrero, H.; Waylen, P.R.; Hill, M.J. Changes in vegetation persistence across global savanna landscapes, 1982–2010. *J. Land Use Sci.* **2016**, *11*, 7–32. [CrossRef]
9. Tropical and subtropical grasslands, savannas and shrublands|Biomes|WWF. Available online: <https://www.worldwildlife.org/biomes/tropical-and-subtropical-grasslands-savannas-and-shrublands> (accessed on 1 May 2020).
10. Ferreira, J.N.; Bustamante, M.M.d.C.; Davidson, E.A. Linking woody species diversity with plant available water at a landscape scale in a Brazilian savanna. *J. Veg. Sci.* **2009**, *20*, 826–835. [CrossRef]
11. Dantas, V.d.L.; Batalha, M.A. Vegetation structure: Fine scale relationships with soil in a cerrado site. *Flora - Morphol. Distrib. Funct. Ecol. Plants* **2011**, *206*, 341–346. [CrossRef]
12. Herrero, H.V.; Southworth, J.; Bunting, E. Utilizing Multiple Lines of Evidence to Determine Landscape Degradation within Protected Area Landscapes: A Case Study of Chobe National Park, Botswana from 1982 to 2011. *Remote Sens.* **2016**, *8*, 623. [CrossRef]
13. Pennington, R.T.; Lehmann, C.E.R.; Rowland, L.M. Tropical savannas and dry forests. *Curr. Biol.* **2018**, *28*, R541–R545. [CrossRef] [PubMed]
14. Southworth, J.; Munroe, D.; Nagendra, H. Land cover change and landscape fragmentation—Comparing the utility of continuous and discrete analyses for a western Honduras region. *Agric. Ecosyst. Environ.* **2004**, *101*, 185–205. [CrossRef]
15. Jensen, J.R. *Introductory Digital Image Processing: A Remote Sensing Perspective*, 4th ed.; Prentice Hall Press: Upper Saddle River, NJ, USA, 2015; ISBN 978-0-13-405816-0.
16. Maximum Likelihood. Available online: <https://www.harrisgeospatial.com/docs/MaximumLikelihood.html> (accessed on 21 May 2020).
17. Support Vector Machine. Available online: <https://www.harrisgeospatial.com/docs/SupportVectorMachine.html> (accessed on 15 June 2020).
18. Decision Tree. Available online: <https://www.harrisgeospatial.com/docs/DecisionTree.html> (accessed on 15 June 2020).
19. Herrero, H.V.; Southworth, J.; Bunting, E.; Kohlhaas, R.R.; Child, B. Integrating Surface-Based Temperature and Vegetation Abundance Estimates into Land Cover Classifications for Conservation Efforts in Savanna Landscapes. *Sensors* **2019**, *19*, 3456. [CrossRef]
20. Vogel, M.; Strohbach, M. Monitoring of savanna degradation in Namibia using Landsat TM/ETM+ data. In Proceedings of the 2009 IEEE International Geoscience and Remote Sensing Symposium, Cape Town, South Africa, 12–17 July 2009; Volume 3, pp. III-931–III-934.

21. Furley, P.A. The nature and diversity of neotropical savanna vegetation with particular reference to the Brazilian cerrados. *Glob. Ecol. Biogeogr.* **1999**, *8*, 223–241. [[CrossRef](#)]
22. Mistry, J. Savannas. *Prog. Phys. Geogr. Earth Environ.* **2000**, *24*, 601–608. [[CrossRef](#)]
23. Furley, P.A. *Savannas: A Very Short Introduction*; Oxford University Press: Oxford, UK, 2016; ISBN 978-0-19-871722-5.
24. Biomes|Conserving Biomes|WWF. Available online: <https://www.worldwildlife.org/biomes> (accessed on 1 May 2020).
25. Garbulsky, M.F.; Paruelo, J.M. Remote sensing of protected areas to derive baseline vegetation functioning characteristics. *J. Veg. Sci.* **2004**, *15*, 711–720. [[CrossRef](#)]
26. Josefsson, T.; Hörnberg, G.; Östlund, L. Long-Term Human Impact and Vegetation Changes in a Boreal Forest Reserve: Implications for the Use of Protected Areas as Ecological References. *Ecosystems* **2009**, *12*, 1017–1036. [[CrossRef](#)]
27. April Sahara, E.; Sarr, D.A.; Van Kirk, R.W.; Jules, E.S. Quantifying habitat loss: Assessing tree encroachment into a serpentine savanna using dendroecology and remote sensing. *For. Ecol. Manag.* **2015**, *340*, 9–21. [[CrossRef](#)]
28. Stuart, N.; Barratt, T.; Place, C. Classifying the Neotropical savannas of Belize using remote sensing and ground survey. *J. Biogeogr.* **2006**, *33*, 476–490. [[CrossRef](#)]
29. Climate Summary—National Meteorological Service of Belize. Available online: <https://www.hydromet.gov.bz/climatology/climate-summary> (accessed on 18 May 2020).
30. Fick, S.E.; Hijmans, R.J. WorldClim 2: New 1-km spatial resolution climate surfaces for global land areas. *Int. J. Climatol.* **2017**, *37*, 4302–4315. [[CrossRef](#)]
31. Harris, I.; Jones, P.D.; Osborn, T.J.; Lister, D.H. Updated high-resolution grids of monthly climatic observations – the CRU TS3.10 Dataset. *Int. J. Climatol.* **2014**, *34*, 623–642. [[CrossRef](#)]
32. Funk, C.; Peterson, P.; Landsfeld, M.; Pedreros, D.; Verdin, J.; Shukla, S.; Husak, G.; Rowland, J.; Harrison, L.; Hoell, A.; et al. The climate hazards infrared precipitation with stations—A new environmental record for monitoring extremes. *Sci. Data* **2015**, *2*, 1–21. [[CrossRef](#)] [[PubMed](#)]
33. Cameron, I.; Stuart, N.; Goodwin, Z. *Savanna Ecosystems Map of Belize 2011: Technical Report*; Darwin Initiative Project 17022; University of Edinburgh: Edinburgh, Scotland, 2011; pp. 5–16.
34. Goodwin, Z.A.; Lopez, G.N.; Stuart, N.; Bridgewater, S.G.M.; Haston, E.M.; Cameron, I.D.; Michelakis, D.; Ratter, J.A.; Furley, P.A.; Kay, E.; et al. A checklist of the vascular plants of the lowland savannas of Belize, Central America. *Phytotaxa* **2013**, *101*, 1–119. [[CrossRef](#)]
35. Donoghue, S.; Furley, P.A.; Stuart, N.; Haggis, R.; Trevaskis, A.; Lopez, G. The nature and spatial variability of lowland savanna soils: Improving the resolution of soil properties to support land management policy. *Soil Use Manag.* **2019**, *35*, 547–560. [[CrossRef](#)]
36. Myers, R.; O'Brien, J.; Morrison, S. *Fire Management Overview of the Caribbean Pine (Pinus caribaea) Savannas of the Mosquitia, Honduras*; The Nature Conservancy: Arlington, VA, USA, 2006; p. 6.
37. Fire Management. Available online: <http://tidebelize.org/fire-management/> (accessed on 17 May 2020).
38. Meerman, J.; Sabido, W. *Central American Ecosystems Map: Belize*; Programme for Belize: Belize City, Belize, 2001.
39. EarthExplorer. Available online: <https://earthexplorer.usgs.gov/> (accessed on 17 June 2020).
40. Measuring Vegetation (NDVI & EVI). Available online: <https://earthobservatory.nasa.gov/features/MeasuringVegetation> (accessed on 18 May 2020).
41. Bai, Z.G.; Dent, D.L.; Olsson, L.; Schaepman, M.E. Proxy global assessment of land degradation. *Soil Use Manag.* **2008**, *24*, 223–234. [[CrossRef](#)]
42. Selva Maya Consortium Soils of Belize. Available online: <https://databasin.org/datasets/21a4f58393904edcbdb1ae031a4c6b68> (accessed on 11 May 2020).
43. Cortes, C.; Vapnik, V. Support-vector networks. *Mach Learn* **1995**, *20*, 273–297. [[CrossRef](#)]
44. Burges, C.J.C. A Tutorial on Support Vector Machines for Pattern Recognition. *Data Min. Knowl. Discov.* **1998**, *2*, 121–167. [[CrossRef](#)]
45. Paneque-Gálvez, J.; Mas, J.-F.; Moré, G.; Cristóbal, J.; Orta-Martínez, M.; Luz, A.C.; Guèze, M.; Macía, M.J.; Reyes-García, V. Enhanced land use/cover classification of heterogeneous tropical landscapes using support vector machines and textural homogeneity. *Int. J. Appl. Earth Obs. Geoinf.* **2013**, *23*, 372–383. [[CrossRef](#)]
46. Silva, G.B.S.; Mello, M.P.; Shimabukuro, Y.E.; Rudorff, B.F.T.; de Castro Victoria, D. Multitemporal classification of natural vegetation cover in Brazilian Cerrado. In Proceedings of the 2011 6th International Workshop on the Analysis of Multi-temporal Remote Sensing Images (Multi-Temp), Trento, Italy, 12–14 July 2011; pp. 117–120.

47. Mitchard, E.T.A.; Flintrop, C.M. Woody encroachment and forest degradation in sub-Saharan Africa's woodlands and savannas 1982–2006. *Philos. Trans. R. Soc. B Biol. Sci.* **2013**, *368*, 20120406. [[CrossRef](#)]
48. Sankaran, M.; Hanan, N.P.; Scholes, R.J.; Ratnam, J.; Augustine, D.J.; Cade, B.S.; Gignoux, J.; Higgins, S.I.; Le Roux, X.; Ludwig, F.; et al. Determinants of woody cover in African savannas. *Nature* **2005**, *438*, 846–849. [[CrossRef](#)]
49. Bowman, D.M.J.S.; Walsh, A.; Milne, D.J. Forest expansion and grassland contraction within a Eucalyptus savanna matrix between 1941 and 1994 at Litchfield National Park in the Australian monsoon tropics. *Glob. Ecol. Biogeogr.* **2001**, *10*, 535–548. [[CrossRef](#)]
50. Tng, D.Y.P.; Murphy, B.P.; Weber, E.; Sanders, G.; Williamson, G.J.; Kemp, J.; Bowman, D.M.J.S. Humid tropical rain forest has expanded into eucalypt forest and savanna over the last 50 years. *Ecol. Evol.* **2012**, *2*, 34–45. [[CrossRef](#)] [[PubMed](#)]
51. Silva, L.C.R.; Sternberg, L.; Haridasan, M.; Hoffmann, W.A.; Miralles-Wilhelm, F.; Franco, A.C. Expansion of gallery forests into central Brazilian savannas. *Glob. Chang. Biol.* **2008**, *14*, 2108–2118. [[CrossRef](#)]
52. *Report For: TIDE Payne's Creek National Park Biodiversity Assessment*; Wildtracks: Belize City, Belize, 2005; pp. 4–18.
53. Hurricanes and Tropical Storms Affecting Belize since 1930. Available online: <http://consejo.bz/weather/storms.html> (accessed on 18 May 2020).
54. Stoddart, D.R. Catastrophic Storm Effects on the British Honduras Reefs and Cays. *Nature* **1962**, *196*, 512–515. [[CrossRef](#)]
55. Murray, M.R.; Zisman, S.A.; Furley, P.A.; Munro, D.M.; Gibson, J.; Ratter, J.; Bridgewater, S.; Minty, C.D.; Place, C.J. The mangroves of Belize: Part 1. distribution, composition and classification. *For. Ecol. Manag.* **2003**, *174*, 265–279. [[CrossRef](#)]
56. Furley, P. Plant ecology, soil environments and dynamic change in tropical savannas. *Prog. Phys. Geogr. Earth Environ.* **1997**, *21*, 257–284. [[CrossRef](#)]
57. Coughenour, M.B.; Ellis, J.E. Landscape and Climatic Control of Woody Vegetation in a Dry Tropical Ecosystem: Turkana District, Kenya. *J. Biogeogr.* **1993**, *20*, 383–398. [[CrossRef](#)]
58. Reed, D.N.; Anderson, T.M.; Dempewolf, J.; Metzger, K.; Serneels, S. The spatial distribution of vegetation types in the Serengeti ecosystem: The influence of rainfall and topographic relief on vegetation patch characteristics. *J. Biogeogr.* **2009**, *36*, 770–782. [[CrossRef](#)]



© 2020 by the authors. Licensee MDPI, Basel, Switzerland. This article is an open access article distributed under the terms and conditions of the Creative Commons Attribution (CC BY) license (<http://creativecommons.org/licenses/by/4.0/>).